

## Tunable Photoluminescence from Graphene Oxide\*\*

Chih-Tao Chien, Shao-Sian Li, Wei-Jung Lai, Yun-Chieh Yeh, Hsin-An Chen, I-Shen Chen, Li-Chyong Chen, Kuei-Hsien Chen, Takashi Nemoto, Seiji Isoda, Mingwei Chen, Takeshi Fujita, Goki Eda, Hisato Yamaguchi, Manish Chhowalla, and Chun-Wei Chen\*

Graphene oxide (GO) is a graphene sheet modified with oxygen functional groups<sup>[1]</sup> in the form of epoxy and hydroxy groups on the basal plane and various other types at the edges.<sup>[1]</sup> It exhibits interesting steady-state photoluminescence (PL) properties.<sup>[2–8]</sup> For example, low-energy fluorescence in red to near infrared (NIR) wavelengths (from 600–1100 nm) has been detected for suspensions and solid thin films of as-synthesized GO.<sup>[2,3]</sup> In addition, broad luminescence from 400 to 800 nm from oxygen plasma-treated, mechanically exfoliated, single-layer graphene sheet has been reported.<sup>[4]</sup> Blue fluorescence with a relatively narrow bandwidth when excited with UV irradiation has also been detected from chemically reduced GO (rGO) and graphene quantum dots.<sup>[5,6]</sup> Recently, chemically modified GO or rGO with *n*-butylamine or Mn<sup>2+</sup> has also demonstrated PL emission at a range of energies.<sup>[9,10]</sup> A detailed explanation of the origin of such variable energy PL in GO has yet to be elucidated. This is partly because the sample preparation and reduction methods varied, making it difficult to compare the results. Herein, we have prepared GO suspensions that

exhibit virtually all of the PL features observed by different groups, through careful and gradual reduction of the GO. The systematic evolution of the electronic structure and comprehensive analysis of steady-state and transient PL along with photoluminescence excitation (PLE) spectroscopy measurements indicate that two different types of electronically excited states are responsible for the observed emission characteristics.

GO was synthesized using the modified Hummers method,<sup>[11]</sup> the details of which have been reported.<sup>[5]</sup> GO usually contains a large fraction of sp<sup>3</sup> hybridized carbon atoms bound to oxygen functional groups, which makes it an insulator. Reduction can be achieved chemically (e.g. hydrazine exposure) or by thermal annealing in inert environments.<sup>[12]</sup> Photothermal reduction of GO can be achieved by exposing GO samples to a Xenon flash in ambient conditions.<sup>[13]</sup> In this study, we prepared aqueous GO solutions and subjected them to steady-state Xe lamp irradiation (500 W) with different exposure times of up to three hours. In contrast to reduction by an instantaneous flash, this method provides a controllable, gradual transformation from GO to rGO, allowing exploration of the PL evolution and emission mechanisms from as-synthesized GO to rGO.

The deoxygenation of GO after reduction was confirmed by X-ray photoelectron spectroscopy (XPS), as shown in Figure 1. The C 1s signals of the original GO can be deconvoluted into signals for the C=C bond in aromatic rings (284.6 eV), C–O bond (286.1 eV), C=O bond (287.5 eV), and C(=O)–OH bond (289.2 eV), in agreement with previous assignments.<sup>[14,15]</sup> Increased sp<sup>2</sup> carbon bonding with increased reduction time can be clearly measured, which

[\*] C. T. Chien, S. S. Li, W. J. Lai, Y. C. Yeh, H. A. Chen, I. S. Chen, Prof. C. W. Chen  
Department of Materials Science and Engineering, National Taiwan University  
No. 1, Sec. 4, Roosevelt Road, Taipei, 10617 (Taiwan)  
E-mail: chunwei@ntu.edu.tw  
Dr. L. C. Chen  
Center for Condensed Matter Sciences, National Taiwan University  
No. 1, Sec. 4, Roosevelt Road, Taipei, 10617 (Taiwan)  
Dr. K. H. Chen  
Institute of Atomic and Molecular Sciences, Academia Sinica  
No. 1, Sec. 4, Roosevelt Road, Taipei, 10617 (Taiwan)  
Dr. T. Nemoto  
Institute for Chemical Research, Kyoto University  
Uji, Kyoto, 611-0011 (Japan)  
Prof. S. Isoda  
Institute for Integrated Cell-Material Sciences, Kyoto University  
606-8501 Kyoto (Japan)  
Prof. M. Chen, Dr. T. Fujita  
WPI Advanced Institute for Materials Research, Tohoku University  
2-1-1 Katahira, Aoba-ku, Sendai, Miyagi, 980-8577 (Japan)  
Dr. G. Eda, H. Yamaguchi, Prof. M. Chhowalla  
Department of Materials Science and Engineering, Rutgers University  
607 Taylor Road, Piscataway, NJ 08854 (USA)

[\*\*] This work is supported by the National Science Council, Taiwan for the project of “Core facilities of novel graphene based materials”. (Project No. NSC 98-2119-M-002-020- and 99-2119-M-002-012-).

Supporting information for this article is available on the WWW under <http://dx.doi.org/10.1002/anie.201200474>.

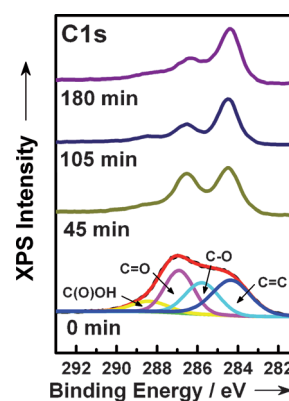
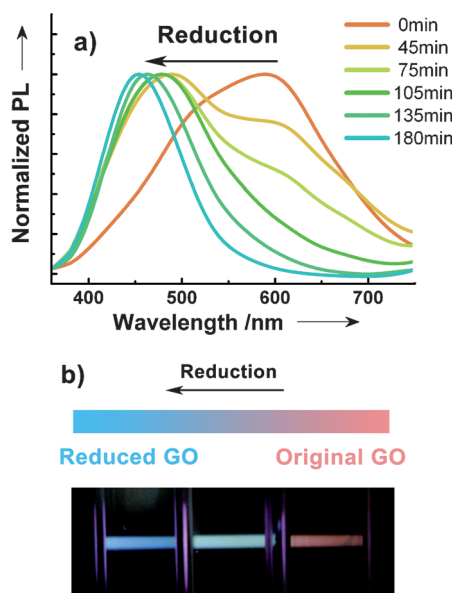


Figure 1. C 1s XPS spectra of GO at different photothermal reduction times. For the deconvoluted signals, C(O)OH (yellow), C=O (purple), C–O (cyan), and C=C (navy blue) were detected.

was accompanied by decreasing peak intensities of the oxygen functional groups. The initial fraction of carbon atoms that were  $sp^2$  bonded ( $C=C$ ) in as-synthesized GO was approximately 25%; this fraction gradually increases with exposure time. A maximum  $sp^2$  carbon fraction of roughly 69% was obtained for the sample that was irradiated for 3 h, slightly lower than that achieved by chemical or ultra high vacuum (UHV) thermal reduction methods.<sup>[14,15]</sup> This difference is because the photothermal reduction used in this case is milder and allows for a gradual transition from GO to rGO.

The evolution of the corresponding normalized PL spectra of GO suspensions with photothermal reduction treatment time is shown in Figure 2a. The PL spectra were obtained by exciting the samples with a continuous wave



**Figure 2.** a) Normalized PL spectra of the GO suspensions after different exposure times (0–180 min) to photothermal reduction treatment. b) Photographs of tunable PL emission from GO at reduction times of 0 min (yellow-red), 75 min (green) and 180 min (blue).

325 nm He–Cd laser (Kimmon Inc.) and the excitation power of the laser was kept low, approximately 5 mW. The typical measurement time for each spectrum was less than 1 minute. No spectral shift was found under the acquisition conditions after 30 minutes without photothermal reduction (see Supporting Information), indicating that the evolution of the PL is a real effect and not an artifact of the measurement system. The as-prepared GO samples showed broad PL, ranging from 400 to 800 nm. The PL peaks gradually move towards shorter wavelengths and narrower bandwidths with reduction, as a function of exposure time. The corresponding photographs of PL from GO solutions at different reduction times are shown in Figure 2b. The colors of PL emission can be gradually tuned from the original yellow-red in the as-synthesized GO solution to the blue in the rGO solution after reduction for 3 h. The corresponding PL spectra of GO suspensions were deconvoluted into two Gaussian-like peaks, labeled as  $I_{P1}$  and  $I_{P2}$ , centered at different wavelengths

(Figure 3a–c). The peak positions and the full widths at half maximum (FWHMs) of  $I_{P1}$  and  $I_{P2}$  emission for GO and rGO samples are shown in Figure 3d,e. The PL of the as-prepared GO was dominated by the  $I_{P1}$  peak centered at approximately

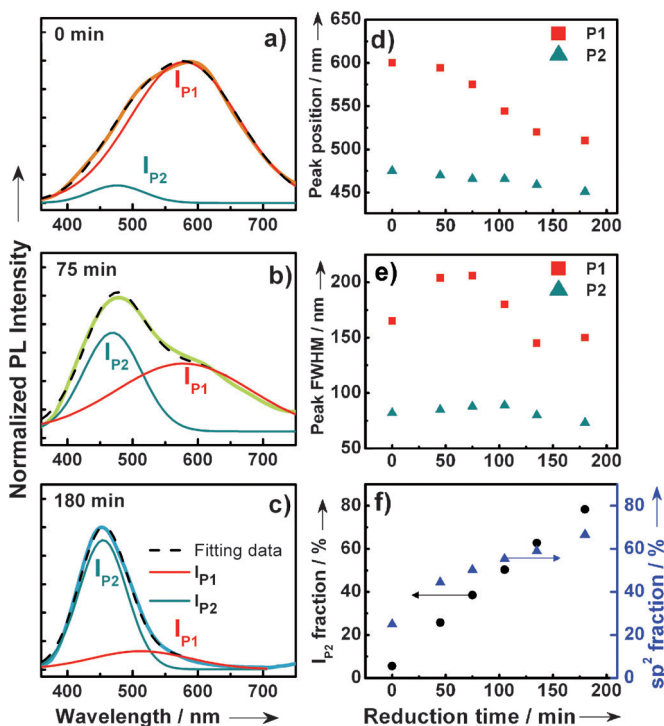


**Figure 3.** PL spectra of a) GO, b) rGO (reduction time = 75 min), and c) rGO (reduction time = 180 min) with two deconvoluted Gaussian-like bands of  $I_{P1}$  and  $I_{P2}$  emission. d) Peak positions and e) the FWHMs of  $I_{P1}$  and  $I_{P2}$  as a function of reduction time. f) Correlation of  $I_{P2}$  fractions (circles) with  $sp^2$  fractions (triangles; from XPS data) with reduction time.

600 nm and a small  $I_{P2}$  emission peak centered at roughly 470 nm. Incremental reduction by increasing exposure times leads to a gradual decrease in the  $I_{P1}$  and a corresponding increase in  $I_{P2}$  emission. The peak position of  $I_{P1}$  was also shifted from 600 nm for the as synthesized GO to 530 nm after 3 h of reduction. In contrast, the peak position of  $I_{P2}$  only shifted slightly to shorter wavelengths with longer reduction time, and rGO exhibited  $I_{P2}$  emission centered at approximately 450 nm, accompanied by a very weak  $I_{P1}$  emission. The increased fraction of  $I_{P2}$  (versus  $I_{P1}$ ) of the integrated PL intensities with reduction time are shown in Figure 3f, which demonstrates a strong correlation with the increased  $sp^2$  fractions calculated from XPS measurements. Accordingly, the evolution of PL emission mainly arises from the varying  $I_{P1}$  to  $I_{P2}$  emission intensity ratios, as a result of the increase in the number of  $sp^2$  carbon atoms.

Next we performed PL excitation (PLE) and time-resolved photoluminescence (TRPL) spectroscopy to examine the electron–hole recombination processes responsible for the  $I_{P1}$  and  $I_{P2}$  emissions. Figure 4a shows the two PLE spectra of the predominantly  $I_{P1}$  emission ( $\lambda_{\text{emission}} = 605$  nm) from the as-synthesized GO and the predominantly  $I_{P2}$  emission

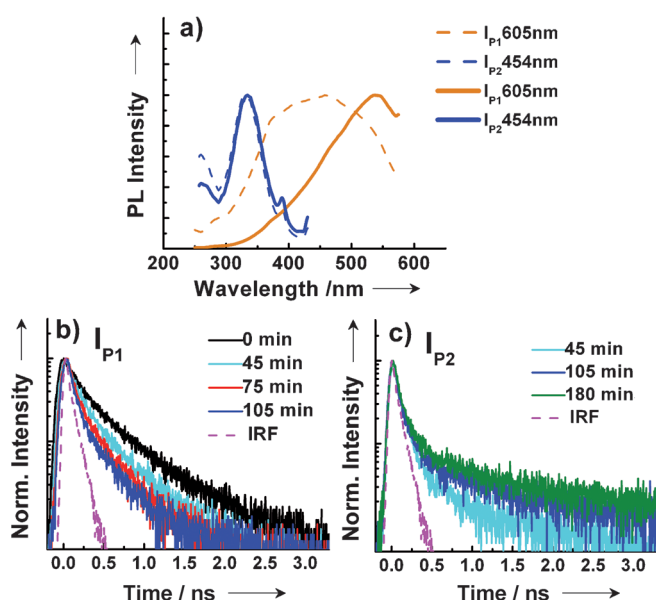


**Figure 4.** a) Measured (dash lines) and normalized (solid lines) PLE spectra of the  $I_{P1}$  emission ( $\lambda_{\text{emission}} = 605$  nm) from as-synthesized GO and the  $I_{P2}$  emission ( $\lambda_{\text{emission}} = 455$  nm) from rGO (reduction for 3 h). The signal at about 375 nm in the excitation spectrum of  $I_{P2}$  emission is the Raman signal of water. The PL transient decay curves of b)  $I_{P1}$  emission and c)  $I_{P2}$  emission at different reduction times.

( $\lambda_{\text{emission}} = 454$  nm) from the rGO sample (reduced for 3 h). To correct the absorption effect, we normalized the measured PLE spectra of GO and rGO samples by dividing their respective absorption coefficients at different excitation wavelengths. The  $I_{P1}$  emission was found over a wide range of excitation wavelengths, from 300 to 570 nm. In contrast, a well-resolved absorption band with a narrow range of excitation wavelengths between 300 and 350 nm was observed for  $I_{P2}$  emission in the rGO sample. Very distinct PLE spectra of  $I_{P1}$  and  $I_{P2}$  emissions indicate that the electron-hole recombination results from different types of electronically excited states for the two cases. Figure 4b,c show the corresponding transient PL decay curves. For the as-prepared GO sample, the dominant  $I_{P1}$  emission shows a multi-exponential PL decay, which can be decomposed into three exponential components of 200, 500, and 1400 ps with various intensity ratios, yielding an average PL decay time of about 600 ps. After photothermal reduction, the PL decay times for the  $I_{P1}$  emission were found to decrease. The PL decay curves of  $I_{P2}$  emission show very different transient behavior. The initial fast decay components of all the rGO samples show a similar temporal response of approximately 100 ps, which is close to the instrumental response function (IRF) of the measurement setup, whereas the PL decay time of the long-lasting tail of  $I_{P2}$  emission was found to increase with reduction time, reaching 1.5 ns for rGO (180 minute reduction). The very different PLE and TRPL results also suggest that the luminescence of  $I_{P1}$  and  $I_{P2}$  emissions arises from two different types of electronically excited states in the heterogeneous electronic structures of GO and rGO.

The atomic structure of GO has been proposed to be a graphene basal plane with a non-uniform coverage of the

oxygen-containing functional groups, resulting in  $sp^2$  carbon clusters of a few nanometers isolated within a defective carbon lattice or the  $sp^3$  matrix.<sup>[12,16,17]</sup> First-principle calculations have also suggested that a large fraction of the C atoms in the hydroxy and epoxy units are bonded to each other to form strips of  $sp^2$  carbon atoms.<sup>[18]</sup> In carbon materials containing a mixture of  $sp^2$  and  $sp^3$  bonding, the optoelectronic properties are mainly determined by the  $\pi$  and  $\pi^*$  states of the  $sp^2$  sites, which lie within the  $\sigma$ - $\sigma^*$  gap.<sup>[18]</sup> Because  $\pi$  bonding is weaker and has lower formation energy, it is expected that a large number of disorder-induced localized states are in the two-dimensional network of as-synthesized GO, which consists of a large fraction of distorted carbon atoms attached to oxygen-containing functional groups. Because the interactions of the  $\pi$  states strongly depend on their projected dihedral angle, the structural disorder-induced localized states may be located in the band tail of the  $\pi$ - $\pi^*$  gap or lie deeper within the gap. As a result, optical transitions between these disorder-induced localized states may cause a broad absorption or emission band (see Supporting Information). The predominant broad  $I_{P1}$  emission band in the as-prepared GO arising from a wide-range of excitation energies may be mainly attributed to optical transitions from these disorder-induced localized states. During deoxygenation by reduction, the number of these disorder-induced states decreases so that the intensity of the  $I_{P1}$  emission is diminished. Meanwhile, the reduction of GO leads to removal of oxygen-containing functional groups, and some of the carbon lattices in the originally distorted  $sp^2$  domains can form new graphitic domains of  $sp^2$  clusters. It has been suggested and experimentally demonstrated that the initially present  $sp^2$  domains in GO do not increase in size with reduction.<sup>[5,12,16]</sup> Instead, the reduction of GO usually leads to the creation of newly formed small  $sp^2$  clusters, which are smaller in size, but numerous. Because the free-energy cost for aromatic clustering would be considerable,<sup>[19]</sup> the disorder potential in the 2D network of GO or rGO is likely to oppose further clustering into large  $sp^2$  domains. These small  $sp^2$  clusters that create the isolated molecular states eventually percolate to mediate the transport of carriers by hopping.<sup>[5]</sup>

To further examine the atomic structure of these small  $sp^2$  clusters, we performed nanoscale morphology analyses of rGO using scanning tunneling microscopy (STM) and high-resolution transmission electron microscopy (HRTEM). Many small  $sp^2$  domains of a few nanometers in size were readily observed in the STM image (Figure 5 a). The arrays of dark dots (shown by arrows) correspond to the crystalline conductive areas of small  $sp^2$  domains in rGO. The pseudo lattice size in these small  $sp^2$  clusters is around 0.4 nm, larger than the typical lattice constant (0.245 nm) of graphene resulting from the rotational moiré pattern between the  $sp^2$  domains in rGO and the highly ordered pyrolytic graphite (HOPG) substrate surface.<sup>[20]</sup> No atomically resolved STM image in the as-synthesized GO sample can be observed because of its highly insulating nature (not shown). Figure 5 b shows the HRTEM image of the rGO sample. An image of one representative small  $sp^2$  cluster with a size of approximately 2 nm consisting of about 50 aromatic rings is also

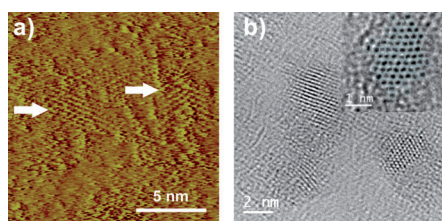


**Figure 5.** a) STM image of rGO with scan size of 15 nm, scan rate of 20 Hz, bias of 4.4 mV, and current of 5 pA. Arrows indicate small  $sp^2$  clusters aligned on the HOPG surface. b) High-resolution TEM image of the rGO. Inset: image of one representative  $sp^2$  cluster.

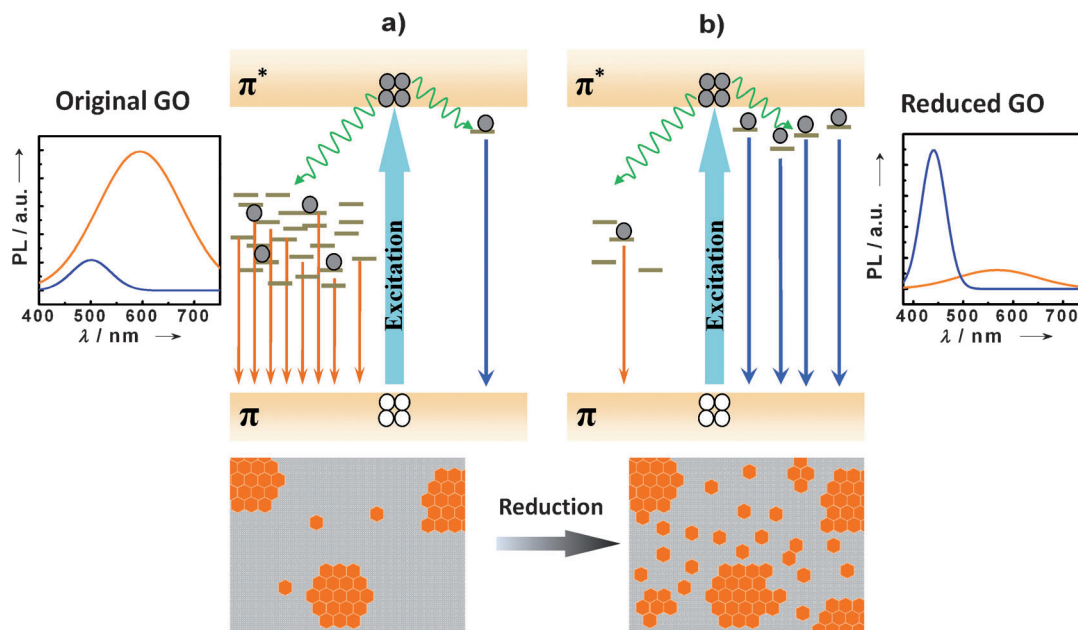
shown in the inset. The electron–hole recombination among the confined cluster states originating from the small and isolated  $sp^2$  domains may lead to excitonic features such as those found in an organic light-emitting molecular semiconductor,<sup>[21]</sup> yielding a narrower emission bandwidth and a well-resolved PLE spectrum as seen with the  $I_{p2}$  emission band. Such excitonic behavior of  $I_{p2}$  emission has been detected in single-walled carbon nanotubes (SWNTs)<sup>[22]</sup> because of the confined geometry but has not been detected in hydrogenated amorphous carbon (a-C:H), where a rather large disorder potential in a 3D network opposes clustering.<sup>[23]</sup> Blue-luminescent graphene quantum dots (GQDs) with sizes less than 10 nm have been reported and the emission from the free zigzag edge sites was proposed as a possible explanation for the fluorescence.<sup>[6,24]</sup> However, we did not find laterally very small GO or rGO sheets in our samples that could be classified as free-standing GQDs (see Supporting Information).

Figure 6 summarizes the mechanisms that explain the evolution of photoluminescence of GO with increased reduction. The original GO consists of numerous disorder-

induced defect states within the  $\pi$ – $\pi^*$  gap and exhibits a broad prominent PL spectrum centered at longer wavelengths, as shown in Figure 6a. After deoxygenation, the number of disorder-induced states within the  $\pi$ – $\pi^*$  gap decreases, and an increased number of cluster-like states from the newly formed small and isolated  $sp^2$  domains are formed, as shown in Figure 6b. The electron–hole recombination among these  $sp^2$  cluster-like states exhibits blue fluorescence at shorter wavelengths with a narrower bandwidth. The tunable PL spectra of GO during reduction are therefore attributed to the variation of the relative intensity ratios of PL emission from two different types of electronically excited states, as a result of changing the heterogeneous electronic structures of GO and rGO with variable  $sp^2$  and  $sp^3$  hybridizations through reduction.

### Experimental Section

For material characterizations, UV/Vis absorption spectra were obtained using a Jasco V570 UV/Vis/NIR spectrophotometer. The PL spectra were obtained by exciting the samples using a continuous wave He–Cd laser at 325 nm (Kimmon Inc.) and the emission spectra were analyzed with a Jobin–Yvon TRIAX 0.55 m monochromator and detected by a photomultiplier tube and standard photocounting electronics. Time-resolved photoluminescence spectroscopy was performed with a time-correlated single photon counting (TCSPC) module (PicoHarp 300, PicoQuant). A pulsed laser (372 nm) with an average power of 1 mW operating at 20 MHz with duration of 70 ps was used for excitation. Photoluminescence excitation (PLE) spectroscopy was measured using a FluoroLog-3 spectrofluorometer (Jobin–Yvon). XPS spectra were obtained using a VG Scientific ESCALAB 250 system. Atomic force microscopy and scanning tunneling microscopy (Nano Scope IIIa, Veeco Inc.) were used to obtain the morphology and atomic-scaled images of GO or rGO deposited on HOPG substrates (ZYH grade, Advanced Ceramic Corporation) using mechanically cut Pt/Ir tips under ambient



**Figure 6.** Proposed PL emission mechanisms of a) the predominant  $I_{p1}$  emission in GO from disorder-induced localized states. b) The predominant  $I_{p2}$  emission in rGO from confined cluster states.

conditions. High-resolution transmission electron microscopy (HRTEM) was performed using JOEL JEM-2100F TEM/STEM with double spherical aberration (Cs) correctors (CEOS GmbH, Heidelberg, Germany) to attain high-contrast images with a point-to-point resolution of 1.4 Å.

Received: January 17, 2012  
Revised: April 11, 2012  
Published online: May 23, 2012

**Keywords:** graphene · graphene oxide · luminescence · materials science · scanning-probe microscopy

- 
- [1] W. W. Cai, R. D. Piner, F. J. Stadermann, S. Park, M. A. Shaibat, Y. Ishii, D. X. Yang, A. Velamakanni, S. J. An, M. Stoller, J. H. An, D. M. Chen, R. S. Ruoff, *Science* **2008**, *321*, 1815.
- [2] X. M. Sun, Z. Liu, K. Welsher, J. T. Robinson, A. Goodwin, S. Zaric, H. J. Dai, *Nano Res.* **2008**, *1*, 203.
- [3] Z. T. Luo, P. M. Vora, E. J. Mele, A. T. C. Johnson, J. M. Kikkawa, *Appl. Phys. Lett.* **2009**, *94*, 111909.
- [4] T. Gokus, R. R. Nair, A. Bonetti, M. Bohmler, A. Lombardo, K. S. Novoselov, A. K. Geim, A. C. Ferrari, A. Hartschuh, *ACS Nano* **2009**, *3*, 3963.
- [5] G. Eda, Y. Y. Lin, C. Mattevi, H. Yamaguchi, H. A. Chen, I. S. Chen, C. W. Chen, M. Chhowalla, *Adv. Mater.* **2010**, *22*, 505.
- [6] D. Y. Pan, J. C. Zhang, Z. Li, M. H. Wu, *Adv. Mater.* **2010**, *22*, 734.
- [7] K. S. Subrahmanyam, P. Kumar, A. Nag, C. N. R. Rao, *Solid State Commun.* **2010**, *150*, 1774.
- [8] J. Lu, J. Yang, J. Wang, A. Lim, S. Wang, K. P. Loh, *ACS Nano* **2009**, *3*, 2367.
- [9] Q. S. Mei, K. Zhang, G. J. Guan, B. H. Liu, S. H. Wang, Z. P. Zhang, *Chem. Commun.* **2010**, *46*, 7319.
- [10] Z. X. Gan, S. J. Xiong, X. L. Wu, C. Y. He, J. C. Shen, P. K. Chu, *Nano Lett.* **2011**, *11*, 3951.
- [11] M. Hirata, T. Gotou, S. Horiuchi, M. Fujiwara, M. Ohba, *Carbon* **2004**, *42*, 2929.
- [12] K. P. Loh, Q. L. Bao, G. Eda, M. Chhowalla, *Nat. Chem.* **2010**, *2*, 1015.
- [13] L. J. Cote, R. Cruz-Silva, J. X. Huang, *J. Am. Chem. Soc.* **2009**, *131*, 11027.
- [14] S. Stankovich, D. A. Dikin, R. D. Piner, K. A. Kohlhaas, A. Kleinhammes, Y. Jia, Y. Wu, S. T. Nguyen, R. S. Ruoff, *Carbon* **2007**, *45*, 1558.
- [15] C. Mattevi, G. Eda, S. Agnoli, S. Miller, K. A. Mkhoyan, O. Celik, D. Mestrogiovanni, G. Granozzi, E. Garfunkel, M. Chhowalla, *Adv. Funct. Mater.* **2009**, *19*, 2577.
- [16] C. Gómez-Navarro, J. C. Meyer, R. S. Sundaram, A. Chuvilin, S. Kurasch, M. Burghard, K. Kern, U. Kaiser, *Nano Lett.* **2010**, *10*, 1144.
- [17] K. A. Mkhoyan, A. W. Contryman, J. Silcox, D. A. Stewart, G. Eda, C. Mattevi, S. Miller, M. Chhowalla, *Nano Lett.* **2009**, *9*, 1058.
- [18] J. Yan, L. Xian, M. Y. Chou, *Phys. Rev. Lett.* **2009**, *103*, 086802.
- [19] J. Robertson, *Adv. Phys.* **1986**, *35*, 317.
- [20] A. Hoshino, S. Isoda, H. Kurata, T. Kobayashi, *J. Appl. Phys.* **1994**, *76*, 4113.
- [21] H. Bässler, M. Gailberger, R. F. Mahrt, J. M. Oberski, G. Weiser, *Synth. Met.* **1992**, *49*, 341.
- [22] S. M. Bachilo, M. S. Strano, C. Kittrell, R. H. Hauge, R. E. Smalley, R. B. Weisman, *Science* **2002**, *298*, 2361.
- [23] J. Robertson, *Phys. Rev. B* **1996**, *53*, 16302.
- [24] J. Peng, W. Gao, B. K. Gupta, Z. Liu, R. Romero-Aburto, L. Ge, L. Song, L. B. Alemany, X. Zhan, G. Gao, S. A. Vithayathil, B. A. Kaiparettu, A. A. Marti, T. Hayashi, J.-J. Zhu, P. M. Ajayan, *Nano Lett.* **2012**, *12*, 844.
-